Available online at www.sciencedirect.com

jmr&t Journal of Materials Research and Technology

journal homepage: www.elsevier.com/locate/jmrt

Original Article

The effect of solution temperature on the precipitates evolution and aging hardening response of Al-15%Mg_2Si(-1%Cu) alloys

Yilin Sun [a], Min Hu [a], Mengran Li [a], Chong Li [a,*], Xiangzhen Zhu [b], Xingchuan Xia [c], Liming Yu [a], Yongchang Liu [a]

[a] State Key Lab of Hydraulic Engineering Simulation and Safety, School of Materials Science and Engineering, Tianjin University, Tianjin, 300354, PR China

[b] Brunel Centre for Advanced Solidification Technology (BCAST), Institute of Materials and Manufacturing, Brunel University London, Uxbridge, Middlesex, UB8 3PH, United Kingdom

[c] School of Material Science and Engineering, Hebei University of Technology, Tianjin, 300130, PR China

ARTICLE INFO

Article history:
Received 17 November 2021
Accepted 18 January 2022
Available online 24 January 2022

Keywords:
Al-Mg_2Si alloy
Solution temperature
Cu addition
Precipitation

ABSTRACT

The effect of solution temperature on the aging hardening behavior of Al-15%Mg_2Si(-1%Cu) alloys was studied by characterizing the precipitation behaviors of nano-precipitates. After the solution temperature rises from 520 °C to 550 °C, more solute atoms are available for precipitation, and the formation activation energies of precipitates (β" and S) decrease. So the formation of β"/β′ in Al-15%Mg_2Si alloy and S in Al-15%Mg_2Si-1%Cu alloy is accelerated at a solution temperature of 550 °C, which enhances the hardness and ultimate tensile strength (UTS) of the two alloys.

1. Introduction

In recent years, the Al-Mg_2Si alloy, reinforced by intermetallic compound Mg_2Si, has an attractive application prospect in automotive manufacturing owing to the advantage of Mg_2Si (high melting point and hardness, low density and thermal expansion coefficient) [1–7]. Moreover, besides Mg_2Si, the intermetallics such as θ phase (Al_2Cu) and Q phase ($Al_5Cu_2Mg_8Si_6$) are also important for strength and ductility of the Al-Mg_2Si alloys after alloyed with Cu [8–10]. These hard intermetallics can not only directly strengthen the alloy, but also dissolve into the Al matrix to provide necessary solute atoms for the precipitation of nano-precipitates during aging heat treatment, thus further improving the strength of the Al-Mg_2Si alloys [9,11].

The β" (Mg_5Si_6, a = 1.516 nm, b = 0.405 nm and c = 0.674 nm), β' (Mg_9Si_5, a = 0.715 nm and c = 1.215 nm) and S (Al_2CuMg, a = 0.4 nm, b = 0.92 nm and c = 0.71 nm) phase (formed after low Cu alloying) are typical nano-precipitates in Al-Mg_2Si (-Cu) alloy system [9,11–13]. These precipitates are

* Corresponding author.
E-mail address: lichongme@tju.edu.cn (C. Li).

https://doi.org/10.1016/j.jmrt.2022.01.094

Table 1 – Actual chemical compositions of two alloys (wt.%).

Alloys	Al	Mg	Si	Cu
Al-15%Mg_2Si	Bal.	9.7	5.5	–
Al-15%Mg_2Si-1%Cu	Bal.	9.8	5.4	1.2

Note: Chemical compositions were detected by inductively coupled plasma mass spectrometry.

assembled by the solute atoms after the solution treatment and are essential for the mechanical properties of the alloys.

However, during solution treatment, the alloys are exposed to high temperatures [14]. The low solution temperature could result in the incomplete dissolution of intermetallic compounds and a decreased level of homogenization. But an excessive solution temperature leads to partial melting of eutectic microstructure. Hence, the solution temperature is an important factor for the strengthening effect. The increased solution temperatures are needed to ensure the solute supersaturation degree without destroying the properties of the alloys [9,15–20].

Therefore, the aging hardening behaviors of as-cast Al-Mg_2Si (1%Cu) alloys with different solution temperatures were studied in the current work by characterizing the formation and precipitation kinetics of nano-precipitates. And it can provide a reference to optimize the heat treatment process of the Al-Mg_2Si (1%Cu) alloys at different solution temperatures.

2. Materials and methods

The preparation of Al-15%Mg_2Si(-1%Cu) alloys (wt.% in this work) was mentioned in our previous paper [9]. The actual chemical compositions of the alloys were listed in Table 1.

The specimens (Φ8 mm × 6 mm) were solution treated for 6 h at 520 or 550 °C, then quenched in cold water and aged in an oil bath at 200 °C for varying periods of time. A macro Vickers hardness tester (ASTM E92-82) with a 200 gf load and a dwell time of 5 s was used to measure hardness value of the specimens with different aging time (the average of ten individual measurements).

The microstructures of as-cast and solution alloys were observed by field emission scanning electron microscope (Hitachi Model No. S4800). The precipitation kinetics of two alloys after quenching were analyzed using differential scanning calorimetry (DSC, Mettler Toledo) from 100 °C to 400 °C with a heating rate of 10 K/min in flowing high purity argon gas.

Twin-jet electropolishing 3 mm discs in a 30% nitric acid 70% methanol solution at −30 °C were used to prepare thin foils for transmission electron microscopy (TEM) and high-resolution TEM (HRTEM). TEM (operated at 120 kV) and HRTEM observations (operated at 200 kV) of nano-precipitates were obtained using an FEI Tecnai F30 microscope. Image Pro plus was used to measure the volume fraction of Mg_2Si phase and the average size of precipitates. Mg_2Si and Al matrix are distinguished by different gray values. The volume fraction of Mg_2Si phase is represented by the average area fraction of Mg_2Si phase (measured more than 10 SEM pictures). The size and number of precipitates can be measured and counted by importing more than ten DM3 files corresponding to the TEM and HRTEM images. The measurement data of more than 50 precipitates are collected to reduce the measurement error. All line charts and histograms in the discussion section were plotted with Origin 8 software.

Tensile tests with a crosshead speed of 0.11 mm/min were performed on three samples (each data value) by using an INSTRON 1342/H1314 at 25 °C.

3. Results and discussion

3.1. Microstructure characterization

Fig. 1 shows the morphology of Al-15%Mg_2Si(-1%Cu) alloys with or without solution treatment. Fig. 1a (d), b (e) and c (f) are corresponding to as-cast, solution treated at 520 °C and 550 °C conditions, respectively. The primary Mg_2Si phases and binary eutectic microstructure exist in Al-15%Mg_2Si alloy

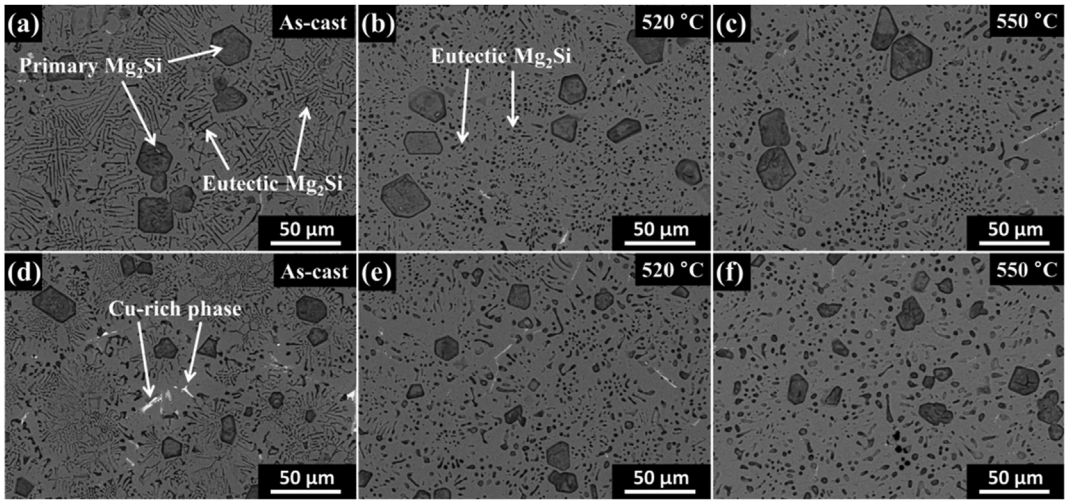

Fig. 1 – The morphology of (a), (b) and (c) Al-15%Mg_2Si and (d), (e) and (f) Al-15%Mg_2Si-1%Cu alloys at different conditions.

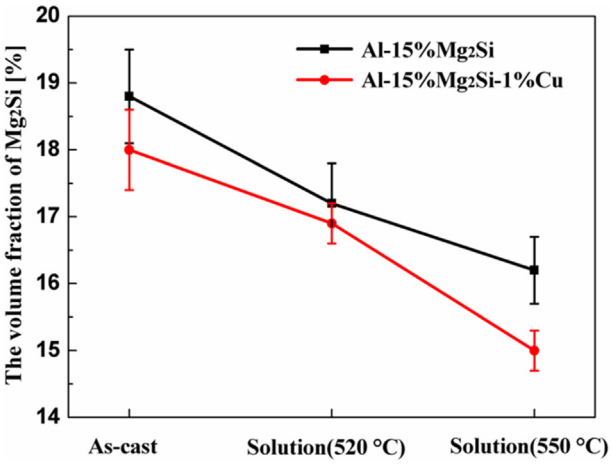

Fig. 2 – The volume fraction of Mg_2Si under different heat treatment conditions.

(Fig. 1a), and Cu-rich phases (θ-Al_2Cu and Q-$Al_5Cu_2Mg_8Si_6$) are formed after the addition of 1%Cu (Fig. 1d) [9]. After the solution treatment at 520 °C or 550 °C for 6 h, sharp corners of primary Mg_2Si and Cu-rich phases dissolve into the matrix, and eutectic Mg_2Si phases are broken into rod-like or spherical morphology, which is reported in the previous studies [21,22].

The volume fraction of Mg_2Si (primary and eutectic) under different heat treatment conditions is presented in Fig. 2. The reduced volume fraction of Mg_2Si with increasing solution temperature indicates that more Mg_2Si phases dissolve into the matrix. The elevated solution temperature causes the increased content of Mg, Si and Cu atoms in the matrix, which can significantly affect the aging process of the alloys.

3.2. *Aging hardening behavior*

After solution-aging treatment, the hardness curves with different solution temperatures are provided in Fig. 3 and corresponding peak hardness values for both alloys are summarized in Table 2. With the solution temperature increasing from 520 °C to 550 °C, the peak hardness increases from 85 HV to 95 HV for Al-15%Mg_2Si alloy and from 121 HV to 144 HV for Al-15%Mg_2Si-1%Cu alloy.

3.3. *Precipitates evolution of Al-15%Mg_2Si(-1%Cu) alloys*

TEM and HRTEM images of the peak-aging condition are shown in Figs. 4 and 5, in order to better understand the age-hardening behavior of the alloys with different solution temperatures.

Fig. 4a exhibits that the β" and β′ phases are formed in Al-15%Mg_2Si alloy under the peak aging condition (solution at 520 °C followed by aging at 200 °C), and the HRTEM images of β" and β′ phases are shown in Fig. 4b and c. For the Al-15% Mg_2Si alloy solution treated at 550 °C, more fine β" and β′ phases are formed (Fig. 4d). The average diameters of β" (decreasing from 3.6 nm to 2.6 nm) and β' (decreasing from 8.4 nm to 5.8 nm) phases reduce significantly, compared with that solution treated at 520 °C (Fig. 6a).

After adding 1%Cu, the type, size and quantity of precipitates changed apparently (Fig. 5). The change of precipitates type (solution at 520 °C) in Al-15%Mg_2Si-1%Cu alloy was reported in our previous work [9]. The alloy exhibits lath-like S precipitates in peak-aging condition (solution at 520 °C) instead of β"/β′ phases (Fig. 5a), owing to the stronger binding energy of Cu and Mg atoms. Fig. 5b shows an HRTEM image of S phase and its FFT spectrum. Because the structure of the S′ phase was believed to be crystallographically similar to that of equilibrium S precipitate, no distinction was made in this work.

Moreover, as shown in Fig. 5a and c, the Al-15%Mg_2Si-1%Cu alloy solution-treated at 550 °C produced more S phases than that solution-treated at 520 °C. With the solution temperature increasing to 550 °C (Fig. 5c and d), the average diameter of S phase decreases from 4.3 nm to 3.5 nm, and the number density increases from 5.85×10^{21} m^{-3} to 7.45×10^{21} m^{-3} (Fig. 6b). The formation of more S phase is responsible for the advanced peak time and higher peak hardness (Fig. 3b).

3.4. *The calculated formation activation energy of precipitates*

Fig. 7 displays DSC curves obtained at a heating rate of 10 K/min of the two alloys solution treated at 520 °C and 550 °C. For Al-15%Mg_2Si alloy, the exothermic peak A between 230 °C and 280 °C, reported as the precipitation of β" phase [23,24]. For Al-

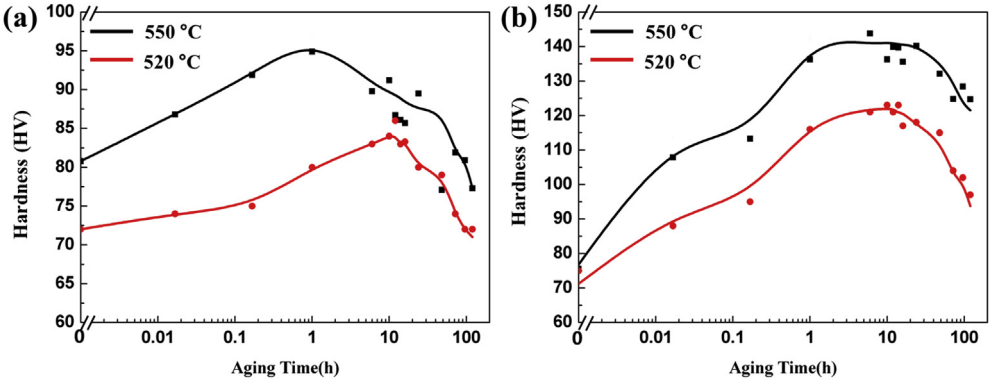

Fig. 3 – Hardness curves of (a) Al-15%Mg_2Si and (b) Al-15%Mg_2Si-1%Cu alloys aging at 200 °C with different solution temperatures.

Table 2 – The peak hardness for both alloys with different solution temperatures.

Alloys	Peak hardness (HV)	
	520 °C	550 °C
Al-15%Mg_2Si	85	121
Al-15%Mg_2Si-1%Cu	95	144

Note: Peak hardness values are obtained from hardness curves (Fig. 3).

15%Mg_2Si-1%Cu alloy, exothermic peak B between 220 °C and 290 °C was considered as the formation of S phase [15,25–27]. It is essential to understand transformation kinetics of two alloys by evaluating the activation energy of precipitation reaction. According to the Johnson-Mehl-Avrami (JMA) model [28–30], the formation activation energy of β'' and S phase can be determined as:

$$Y = 1 - \exp(-kt^n), \quad (1)$$

$$k = k_0 \exp(-Q/RT), \quad (2)$$

where k is the temperature correlation coefficient. k_0 and R are constants. n (a value of 1.5 used for aluminum [28]) is the nucleation growth coefficient. Q is the precipitation activation energy. Y (obtained from DSC curves) is the volume fraction of precipitates at T [28,31].

By derivation of Eq. (1) to t, the transformation rate of volume fraction is shown as:

$$dY/dt = k^{1/n} f(Y), \quad (3)$$

where $f(Y)$ is a function of Y.

$$f(Y) = n(1-Y)(-\ln(1-Y))^{n-1/n}. \quad (4)$$

Based on Eqs. (2)–(4),

$$\ln[(dY/dT)(\Phi/f(Y))] = (1/n)\ln k_0 - Q/(nRT), \quad (5)$$

where Φ is heating rate (10 K/min). The variations of $\ln[(dY/dT)(\Phi/f(Y))]$ with 1/T are plotted at different solution temperatures to estimate the formation activation energy of precipitates. Based on the slop (Q/nR) of the fitted straight lines (found by least-square fitting in Fig. 8), the Q of precipitates can be calculated.

The formation activation energies of β'' (decreasing from 102.5 kJ/mol to 98.4 kJ/mol) and S phases (decreasing from 81.7 kJ/mol to 76.1 kJ/mol) decrease with solution temperature increasing. The reduced formation activation energies of precipitates reflect the accelerated aging kinetics in two alloys. Nano-precipitates have high precipitation potential at elevated solution temperatures due to the increased supersaturation degree and decreased thermal diffusion activation energies of solute atoms [15], which promotes forming more precipitates with finer size (β'', β′ and S phases), as shown in Fig. 6.

In addition, mismatch strains are formed after quenching from the high temperature due to the large thermal expansion coefficient difference between the Al matrix (~26.6 × 10^{-6}/°C)

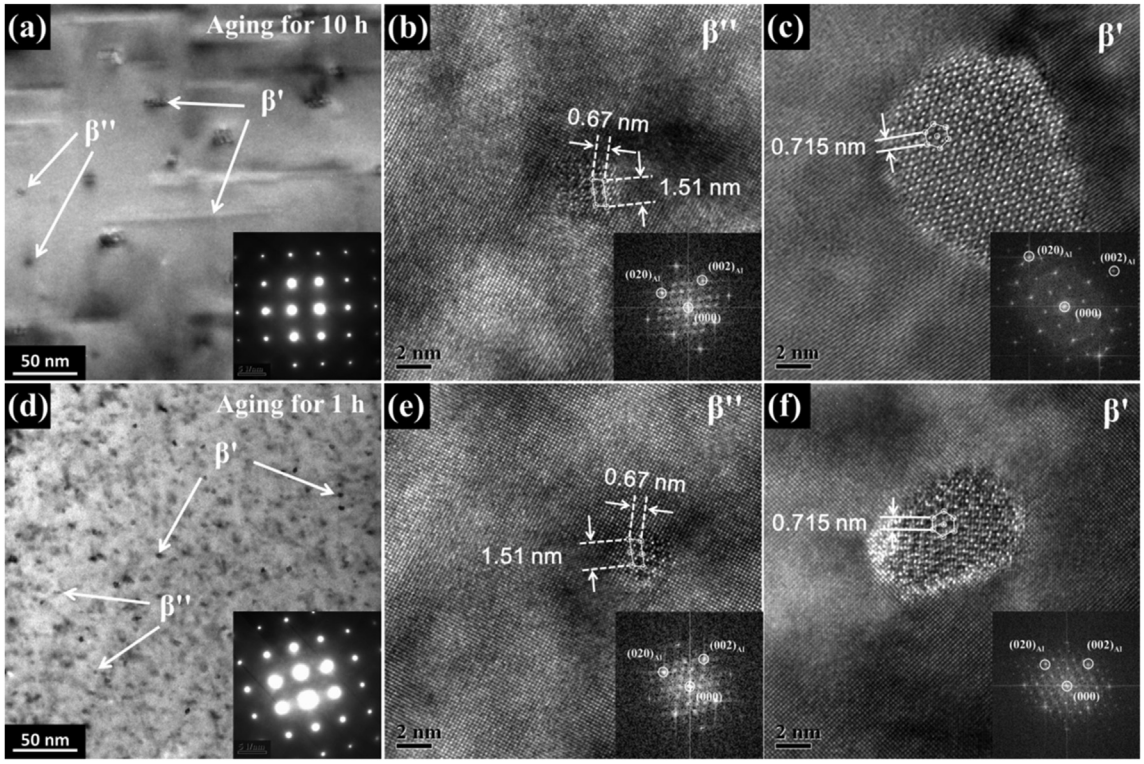

Fig. 4 – Bright-field TEM images with corresponding selected-area electron diffraction (SAED) patterns recorded near <100>$_{Al}$ and HRTEM images with fast Fourier transformation (FFT) spectrum of β'' and β′ phase in peak-aged Al-15%Mg_2Si alloy: at a solution temperature of (a) (b) (c) 520 °C and (d) (e) (f) 550 °C.

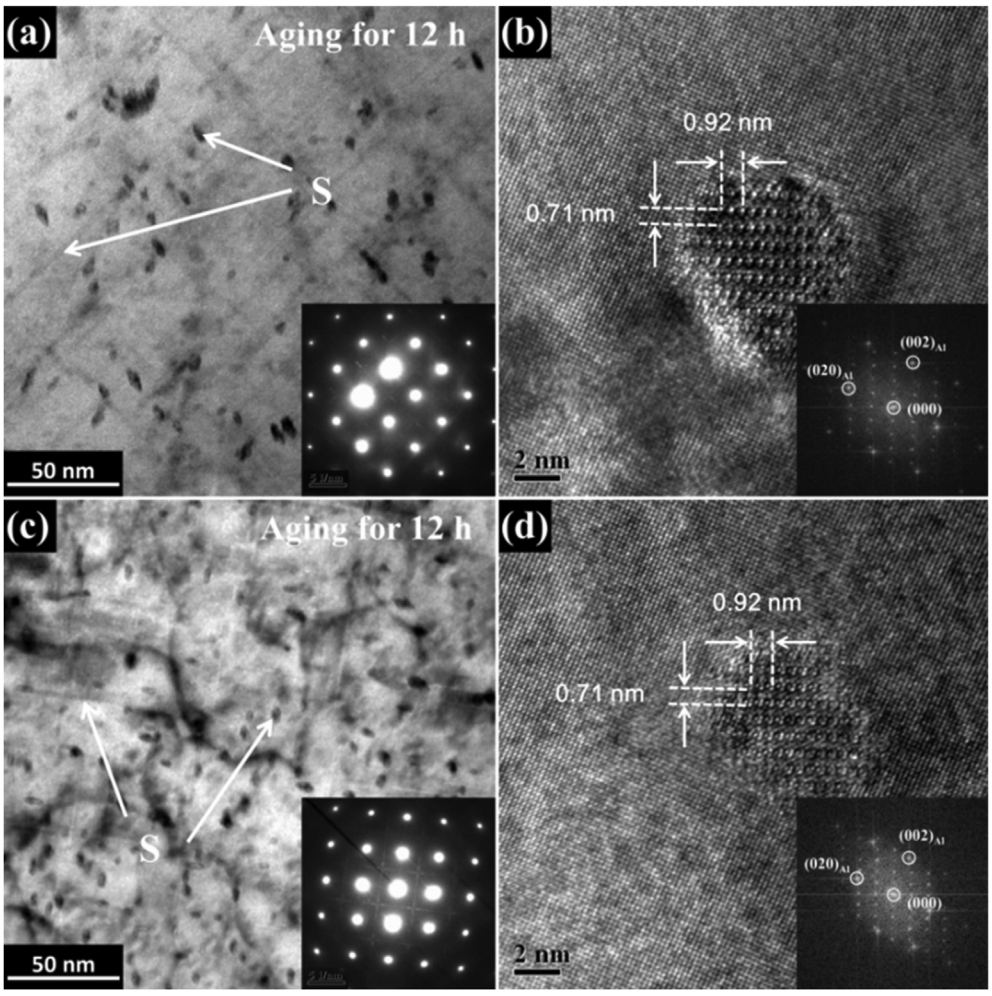

Fig. 5 – Bright-field TEM images with SAED patterns recorded near <100>$_{Al}$ and corresponding HRTEM image with FFT spectrum of S phase in peak-aged Al-15%Mg_2Si-1%Cu alloy: at a solution temperature of (a) (b) 520 °C and (c) (d) 550 °C.

and Mg_2Si phase (~7.5 × 10^{-6}/°C). These mismatch strains can promote the formation of dislocations and provide heterogeneous nucleation sites for nano-precipitates [32–34], as shown in Fig. 9. Moreover, the alloy with a higher solution temperature promotes more dislocations around Mg_2Si after quenching (Fig. 9b). This high-density dislocation is also the important reason for the finer precipitates and decreased formation activation energy.

3.5. *Mechanical properties*

Fig. 10 presents the ultimate tensile strength (UTS) of peak-aging alloys with different solution temperatures. For two alloys, the strength of peak aging alloys increases with solution temperature increasing. Firstly, the modified morphology and reduced sharp corners (nucleation sites for cracks) of Mg_2Si after solution treatment lead to the improved strength of the

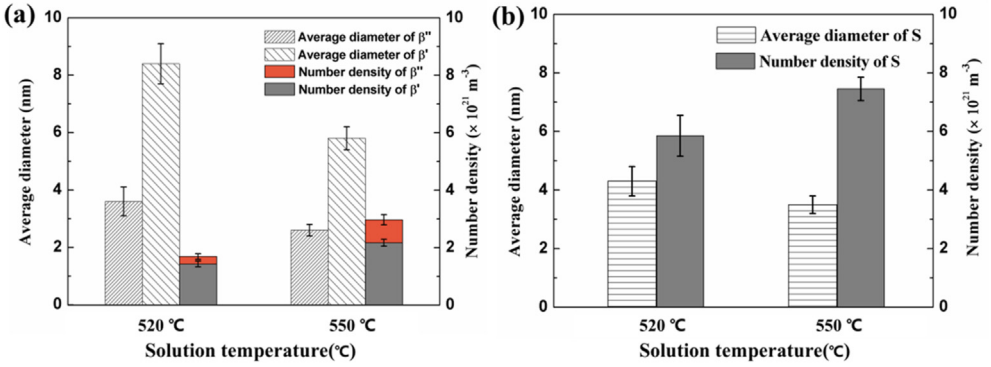

Fig. 6 – Average diameter and number density of (a) β''/β′ and (b) S phase in Al-15%Mg_2Si(-1%Cu) alloys under peak-aging conditions.

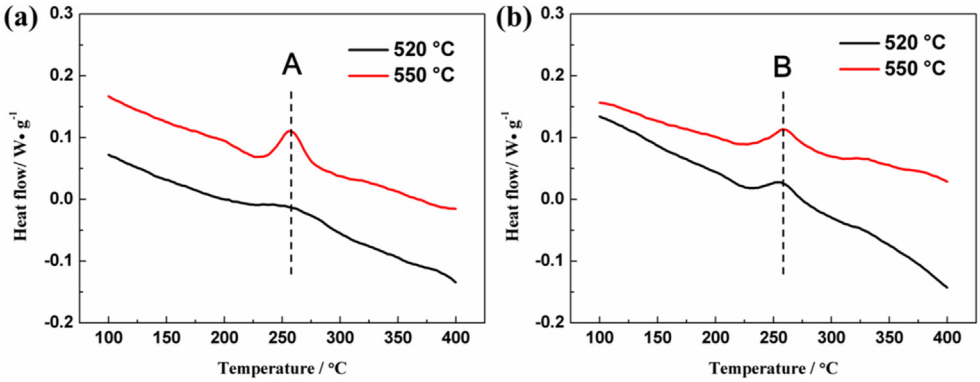

Fig. 7 – DSC curves of solution (a) Al-15%Mg_2Si and (b) Al-15%Mg_2Si-1%Cu alloys quenched at 520 °C and 550 °C.

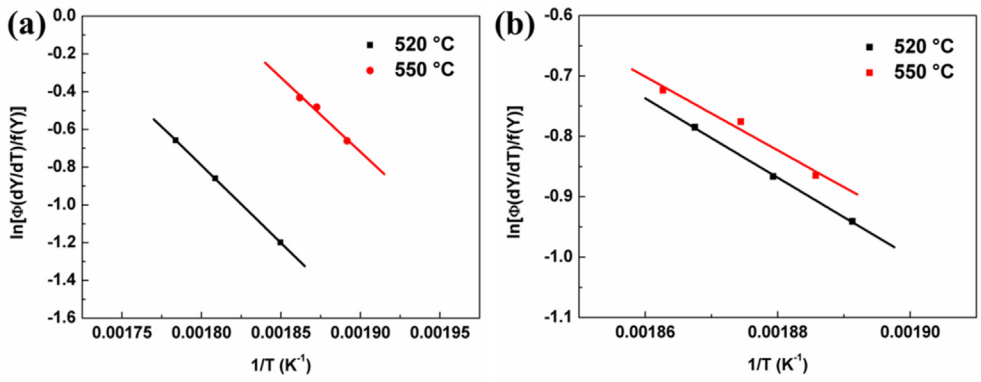

Fig. 8 – Fitting lines of calculated activation energies of (a) β'' phase in Al-15%Mg_2Si alloy and (b) S phase Al-15%Mg_2Si-1%Cu alloy.

alloy (Fig. 1). Secondly, mismatch strains and high-density dislocation around the Mg_2Si (large linear expansion coefficient difference with Al matrix) after quenching also promote the strengthening of the alloy (Fig. 9). Most importantly, for aging hardening alloy, the nano-precipitates formed during aging can hinder the dislocation movement and provide strengthening for the alloy [15,23,25]. The dispersed precipitates (β''/β′ and S phases in Figs. 4 and 5) uniformly distributed can significantly promote the age-hardening process and strengthening effect of the alloys. Therefore, as solution treatment temperature rises from 520 °C to 550 °C, the UTS is improved from 186 MPa to 249 MPa for Al-15%Mg_2Si alloy and from 283 MPa to 334 MPa for Al-15%Mg_2Si-1%Cu alloy.

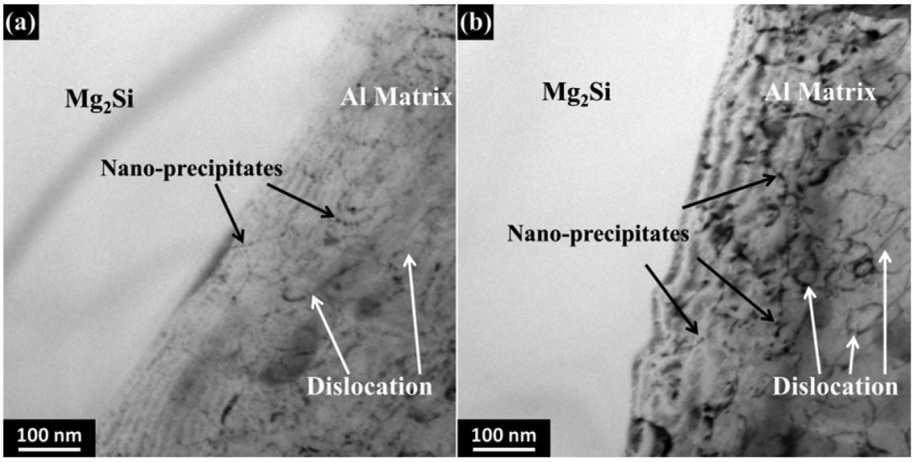

Fig. 9 – Bright-field TEM images at peak-aging condition in Al-15%Mg_2Si alloy with different solution temperature: (a) 520 °C and (b) 550 °C.

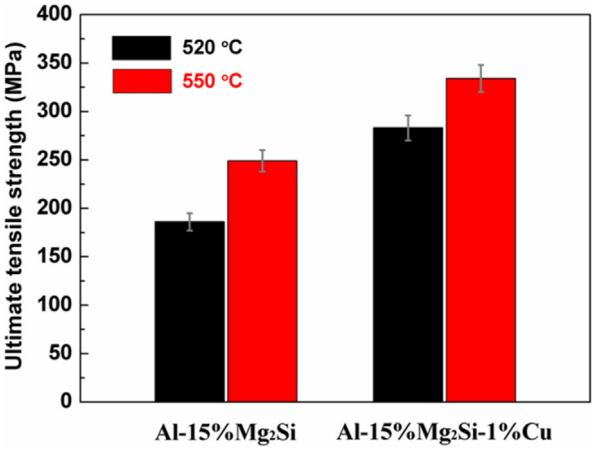

Fig. 10 – Ultimate tensile strength of peak aging Al-15% Mg_2Si(-1%Cu) alloys with different solution temperatures at 25 °C.

4. Conclusion

Solution temperature has an obvious effect on precipitates formation and age-hardening behavior of Al-15%Mg_2Si(-1% Cu) alloys. The increased solution temperature (from 520 °C to 550 °C) can reduce the formation activation energies of precipitates (β" and S). As a result, the formation of β"/β′ phases in Al-15%Mg_2Si and S phase in Al-15%Mg_2Si-1%Cu is promoted. The fine size and high number density of β"/β′ or S phase are mainly responsible for the improved hardness and ultimate tensile strength of two alloys at a solution temperature of 550 °C.

Declaration of Competing Interest

The authors declare that they have no known competing financial interests or personal relationships that could have appeared to influence the work reported in this paper.

Acknowledgments

This work was supported by a grant from National Natural Science Foundation of China (No. 52122409) and Natural Science Foundation of Tianjin City (No. 20JCYBJC00950).

REFERENCES

[1] Qin Q, Zhao H, Zhang Y, Li J, Wang Z. Microstructures and mechanical properties of Al-Mg_2Si-Si alloys resistance spot welded with Al-Si interlayers. J Mater Res Technol 2019;8:4318–32.
[2] Biswas P, Mandal D, Mondal MK. Failures analysis of in-situ Al-Mg_2Si composites using actual microstructure based model. Mater Sci Eng, A 2020;797:140155.
[3] Ghandvar H, Idris MH, Abu Bakar TA, Nafari A, Ahmad N. Microstructural characterization, solidification characteristics and tensile properties of Al-15%Mg_2Si-x(Gd-Sb) in-situ composite. J Mater Res Technol 2020;9:3272–91.
[4] Hu M, Sun YL, He JC, Li C, Li HJ, Yu LM, et al. Hot deformation behaviour and microstructure evolution of Al-3%Mg_2Si alloy. Mater Char 2022;183:111623.
[5] Zhang X, Yang Y, Jin H, Sui Y, Jiang Y, Wang Q. Effect of Lanthanum content on microstructure and mechanical properties of Al-5Mg-2Si-0.6Mn alloy in squeeze casting. J Mater Res Technol 2021;9:4230–40.
[6] Wang D, Zhang H, Nagaumi H, Jia P, Cui J. Microstructural homogeneity, mechanical properties, and wear behavior of in situ Mg_2Si particles reinforced Al-matrix composites fabricated by hot rolling. J Mater Res Technol 2020;9:1882–92.
[7] Ghandvar H, Jabbar KA, Idris MH, Ahmad N, Jahare MH, Rahimian Koloor SS, et al. Influence of barium addition on the formation of primary Mg_2Si crystals from Al-Mg-Si melts. J Mater Res Technol 2021;11:448–65.
[8] Farahany S, Nordin NA, Ourdjini A, Abu Bakar T, Hamzah E, Idris MH, et al. The sequence of intermetallic formation and solidification pathway of an Al-13Mg-7Si-2Cu in-situ composite. Mater Char 2014;98:119–29.
[9] Li M, Sun Y, Li C, Dong J, Yu L, Liu Y. Effect of Cu addition on precipitation and age-hardening response of an Al-15%Mg_2Si alloy. Mater Char 2020;169:110611.
[10] Chong X, Jiang W, Zhao Y, Xu X, Pan D, Wang Y, et al. High performance of T6-treated Al-15Mg_2Si-3Cu composite reinforced with spherical primary Mg_2Si after the Co-modification of Bi plus Sr. Adv Eng Mater 2019;21:1801119.
[11] Chen L, Yuan S, Kong D, Zhao G, He Y, Zhang C. Influence of aging treatment on the microstructure, mechanical properties and anisotropy of hot extruded Al-Mg-Si plate. Mater Des 2019;182:107999.
[12] Lu G, Sun B, Wang J, Liu Y, Liu C. High-temperature age-hardening behavior of Al–Mg–Si alloys with varying Sn contents. J Mater Res Technol 2021;14:2165–73.
[13] Weng Y, Ding L, Zhang Z, Jia Z, Wen B, Liu Y, et al. Effect of Ag addition on the precipitation evolution and interfacial segregation for Al-Mg-Si alloy. Acta Mater 2019;180:301–16.
[14] Jang JH, Nam DG, Park YH, Park IM. Effect of solution treatment and artificial aging on microstructure and mechanical properties of Al-Cu alloy. T. Nonferr. Metal. Soc. 2013;23:631–5.
[15] Jin P, Xiao BL, Wang QZ, Ma ZY, Liu Y, Li S. Effect of solution temperature on aging behavior and properties of SiCp/Al-Cu-Mg composites. Mater Sci Eng, A 2011;528:1504–11.
[16] Malekan A, Emamy M, Rassizadehghani J, Emami AR. The effect of solution temperature on the microstructure and tensile properties of Al-15%Mg_2Si composite. Mater Des 2011;32:2701–9.
[17] Chiu YC, Du KT, Bor HY, Liu GH, Lee SL. The effects of Cu, Zn and Zr on the solution temperature and quenching sensitivity of Al-Zn-Mg-Cu alloys. Mater Chem Phys 2020;247:122853.
[18] Moshtaghi M, Safyari M, Hojo T. Effect of solution treatment temperature on grain boundary composition and environmental hydrogen embrittlement of an Al-Zn-Mg-Cu alloy. Vacuum 2021;184:109937.
[19] Wang Z, Jiang H, Li H, Li S. Effect of solution-treating temperature on the intergranular corrosion of a peak-aged Al-Zn-Mg-Cu alloy. J Mater Res Technol 2020;9:6497–511.
[20] Zhou P, Song Y, Hua L, Lin J, Lu J. Using novel strain aging kinetics models to determine the effect of solution temperature on critical strain of Al-Zn-Mg-Cu alloy. J Alloys Compd 2020;838:155647.
[21] Sun Y, Li C, Liu Y, Yu L, Li H. Intermetallic phase evolution and strengthening effect in Al-Mg_2Si alloys with different Cu/Ni ratios. Mater Lett 2018;215:254–8.

[22] Sun Y, Li C, Yu L, Gao Z, Xia X, Liu Y. Corrosion behavior of Al-15%Mg_2Si alloy with 1% Ni addition. Results Phys 2020;17:103129.
[23] Ding L, He Y, Wen Z, Zhao P, Jia Z, Liu Q. Optimization of the pre-aging treatment for an AA6022 alloy at various temperatures and holding times. J Alloys Compd 2015;647:238–44.
[24] Kim J, Kobayashi E, Sato T. Influence of natural aging time on two-step aging behavior of Al-Mg-Si(-Cu) alloys. Mater Trans 2015;56:1771–80.
[25] Rodrigo P, Poza P, Utrilla MV, Urena A. Identification of sigma and Omega phases in AA2009/SiC composites. J Alloys Compd 2009;482:187–95.
[26] Hong T, Li X, Wang H, Chen D, Wang K. Effects of TiB_2 particles on aging behavior of in-situ TiB_2/Al-Cu-Mg composites. Mater Sci Eng, A 2015;624:110–7.
[27] Wang SC, Starink MJ. Two types of S phase precipitates in Al-Cu-Mg alloys. Acta Mater 2007;55:933–41.
[28] Li H, Yan Z, Cao L. Bake hardening behavior and precipitation kinetic of a novel Al-Mg-Si-Cu aluminum alloy for lightweight automotive body. Mater Sci Eng, A 2018;728:88–94.
[29] Wu YP, Ye LY, Jia YZ, Liu L, Zhang XM. Precipitation kinetics of 2519A aluminum alloy based on aging curves and DSC analysis. T. Nonferr. Metal. Soc. 2014;24:3076–83.
[30] Irani M, Lim S, Joun M. Experimental and numerical study on the temperature sensitivity of the dynamic recrystallization activation energy and strain rate exponent in the JMAK model. J Mater Res Technol 2019;8:1616–27.
[31] Starink MJ. Analysis of aluminium based alloys by calorimetry: quantitative analysis of reactions and reaction kinetics. Int Mater Rev 2004;49:191–226.
[32] Yin D, Xiao Q, Chen Y, Liu H, Yi D, Wang B, et al. Effect of natural ageing and pre-straining on the hardening behaviour and microstructural response during artificial ageing of an Al-Mg-Si-Cu alloy. Mater Des 2016;95:329–39.
[33] Sun Y, Li C, Liu Y, Ding R, Liu X, Kim S-H, et al. The contribution of aluminides to strength of Al-Mg_2Si-Cu-Ni alloys at room and elevated temperatures. Mater Sci Eng, A 2021;817:141381.
[34] Dong SL, Mao JF, Yang DZ, Cui Y, Jiang LT. Age-hardening behavior of a SiCw/Al-Li-Cu-Mg-Zr composite. Mater Sci Eng, A 2002;327:213–23.